

# INTERNATIONAL SOCIETY FOR SOIL MECHANICS AND GEOTECHNICAL ENGINEERING



*This paper was downloaded from the Online Library of the International Society for Soil Mechanics and Geotechnical Engineering (ISSMGE). The library is available here:*

<https://www.issmge.org/publications/online-library>

*This is an open-access database that archives thousands of papers published under the Auspices of the ISSMGE and maintained by the Innovation and Development Committee of ISSMGE.*

*The paper was published in the proceedings of the 7<sup>th</sup> International Conference on Earthquake Geotechnical Engineering and was edited by Francesco Silvestri, Nicola Moraci and Susanna Antonielli. The conference was held in Rome, Italy, 17 - 20 June 2019.*

# Low pressure grouting with nanosilicate to reduce the liquefaction susceptibility of sand

E. Salvatore, M.C. Mascolo, R. Proia & G. Modoni  
*University of Cassino and Southern Lazio, Cassino, Italy*

D. Grassi  
*BASF Chemicals*

**ABSTRACT:** The severe damages on buildings and infrastructures induced by earthquake liquefaction has highlighted the importance of implementing reliable techniques to reduce the susceptibility of loose sandy deposits beneath new or existing buildings. In this direction, the present paper presents the results of an experimental campaign aimed at analyzing the effectiveness of low-pressure grouting of sand with nanosilicate to mitigate the effects of liquefaction. Sandy specimens, reconstituted at two initial relative densities have been treated with grout prepared with silica content ranging from 1.2% to 5.0% by weight, cured for different periods and have then been subjected to different physical and mechanical tests. The results reveal a lower tendency of the treated material to accumulate excess pore pressures during undrained cyclic loading, proving in this way that the technique can be successfully adopted to mitigate the effects of liquefaction of loose sandy deposits.

## 1 INTRODUCTION

The effects of liquefaction on human establishments, cities, infrastructural networks and industrial districts, may determine a significant damage to the communities with relevant economic repercussions (*e.g.* San Francisco, 1906 - Niigata, 1964 - Anchorage, 1964 - Kocaeli, 1999 - Christchurch, 2011 - Emilia Romagna, 2012).

When the shear waves induced by earthquakes strike loose saturated sandy deposits, especially if the water drainage is prevented by the presence of an upper confining finer crust, the pore pressure may equalize the total stress acting into the material. Thereafter, the contact forces between grains become negligible and the soil starts to behave like a liquid, losing its capability to sustain upper loads.

For structures present at the ground level, the differential settlements induced by the inhomogeneous nature of the soil, drainage conditions and distribution of loads may result intolerable for the building performance and undermine serviceability and safety.

A strategy to avoid this effect consists in adopting piled foundations connecting the superstructure to deeper competent strata, in order to bypass the liquefiable layer or creating a system of lattice walls made of jet grouting (Yamauchi *et al.*, 2017), deep soil mixing (Nguyen *et al.*, 2012) or stone columns (D'Appolonia, 1954). Apart from sustaining the superstructure, these reinforcements produce the effect of reducing the shear deformation of the soil and thus the volumetric coupling responsible for the triggering of liquefaction.

Other methods consist in the massive densification of the soil by means of dynamic compaction (Mayne, 1984), vibratory techniques (Kirsch and Kirsch, 2016) or blasting (Lyman, 1942).

However, all the above techniques are not suitable for existing structures, for which less invasive solutions must be adopted. Injection of microfine cement or chemical product represent a possible solution without inducing significant disturbance to the upper structure.

The development of nanotechnologies has provided new versatile materials for a wide range of scopes in civil engineering. Among them, the nanosilica, mainly commercialized as a water suspension of silica nanoparticles, has been successfully adopted to prevent piping induced by tunneling excavations in highly permeable aquifers. Thanks to its low viscosity, similar to that of water, the grout can penetrate relatively low permeability soils (*e.g.* silty sand) even under low hydraulic gradients and cover large distances. A sodium chloride solution is mixed with the silica during the injection to activate a controlled process that leads to the formation of a gel. The filling of soil pores with this gel is here considered as a possible measure to limit the volumetric contraction upon cyclic shearing and defuse the triggering of liquefaction.

In this paper the effectiveness of the low-pressure injection grouting for reducing the liquefaction susceptibility of a sand is experimentally studied with a series of laboratory tests. The studied sand is firstly characterized by means of a series of undrained cyclic triaxial tests carried out at different cyclic stress amplitudes on samples artificially formed at different densities. Then the same experiments have been performed on similar samples treated with different compositions of silica grout, *i.e.* changing the proportions between silicate, sodium chlorite activator and water. SEM observations and X ray diffractions have been also carried out to interpret the basic mechanisms activated by the technique.

## 2 THE STUDIED MATERIALS

### 2.1 Sand

The studied sand is extracted from the quarry of Fossanova (Priverno, Italy) and serves mainly for industry of glass production. The sand, characterized by sub rounded grains, is currently used as a reference material in the laboratory of University of Cassino and Southern Lazio (*e.g.* Salvatore *et al.*, 2017). The tested material (named S3) is obtained sieving the particles passing the sieve #40 (0.425mm) and retained by the sieve #80 (0.180mm) of the ASTM D422 series. From the physical viewpoint, the material is characterized by a specific gravity of 2.65, a mean diameter of 0.303mm, a coefficient of uniformity of 1.6. Samples are formed at two different states with void ratios ranging between 0.476 and 0.821, pluviating the sand in a mold or tamping with a weight respectively.

The chemical composition of the sand, reported in Table 1 and confirmed by the performed x-ray diffraction test (XRD) (see Figure 1), reveals a major presence of quartz with a few inclusions of metals. In particular, the diffraction planes detected with the x-ray diffractometry show the presence of silicone oxide and minor compounds of muscovite  $KAl_3Si_3O_{10}(OH)_2$  and microcline  $KAlSi_3O_8$ .

### 2.2 Nanosilica grout

The silica used in the present study is a colloidal water suspension with a silica content of 15% in weight. Marketed by BASF Chemicals with the commercial name of MasterRoc-MP325. It is composed of nanoparticles having diameters ranging from 2nm to 100nm. The suspension, stabilized at a pH equal to 10 by means of  $Na^+$  ions, presents a low viscosity (10mPa s). When the product is mixed with an activator, an aqueous solution of NaCl with pH equal to 7 has been adopted in this case, the decay of pH triggers the formation of a gel composed by long

Table 1. Chemical composition of the Fossanova sand S3.

Compound	Concentration by volume (%)
Silicon oxide ( $SiO_2$ )	90.00-96.00
Alumina ( $Al_2O_3$ )	1.35 min
Iron oxide ( $Fe_2O_3$ )	0.13 max
Potassium oxide ( $K_2O$ )	1.10 max

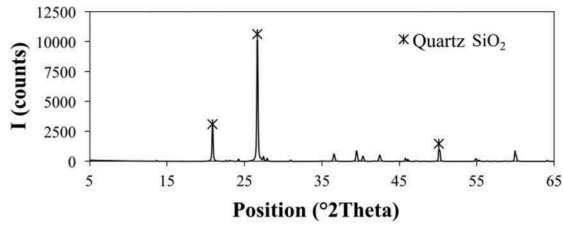


Figure 1. XRD chart of Fossanova sand S3.

hydrophilic chains of silica particles that remain substantially stable along with time (Yonekura, 1996).

The kinematics of the gelling process may be controlled by adjusting the proportions between product and activator and obtain in this way gelling times variable from a few minutes to several hours. This effect has a noticeable relevance for applications as is tightly connected with the extension of the treated portion of material.

Nanosilicates are extensively used as a fast remediation against piping in tunneling (*e.g.* Traldi and Levanto, 2016) or for the sealing of contaminants confining barriers (*e.g.* Persoff *et al.*, 1994; Moridis *et al.*, 1995). However, past studies have also demonstrated the effectiveness of nano-silica grout to reduce the liquefaction potential of sandy soils (Gallagher, 2002; Liao *et al.*, 2003). However, while in these experiments grout mixtures with high fractions of colloidal silica were used, in the present experimental study, lower concentrations are investigated with the twofold scope of considering the unavoidable dilution occurring with grouting in saturated sands and of optimize the technique making it more appealing from the economical viewpoint.

Considering its paramount importance for the in situ applications, a study on the gelling time has been initially performed. Therefore, product and accelerator have been mixed together with different proportions in a small cylindrical container and left at the laboratory environmental conditions ( $T=20^{\circ}\text{C}$ ) for curing. The variation of the gelling time, defined as the time necessary for the grout to remain in the container when this last is overturned, is plotted versus the concentration of activator in Figure 2.

The gelling curve confirms the importance of controlling the amount of activator and the dilution of nanosilicate. Large quantities of the salty solution may in fact complete gelling within few minutes or even less, thus reducing the diffusive capability of the injected grout. On the other hand, lower fractions of the activator may enhance the dispersion of nanosilicates in the natural pore water and reduce the effectiveness of treatment.

In order to study the composition and the morphology of the silica gel, XRD and SEM imaging are performed on small sample of the material. In Figure 3a, the XRD results shown a wide range of diffraction planes around  $22^{\circ}$  revealing the amorphous nature of the gel with some peaks corresponding to sodium chloride (Halite) coming from the activator. The same

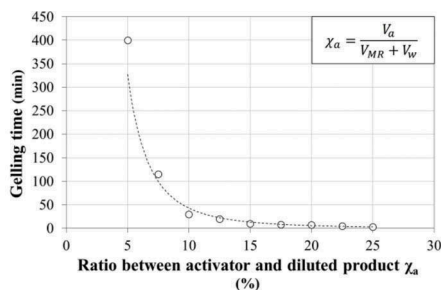


Figure 2. Gelling time versus volume concentration of the activator.

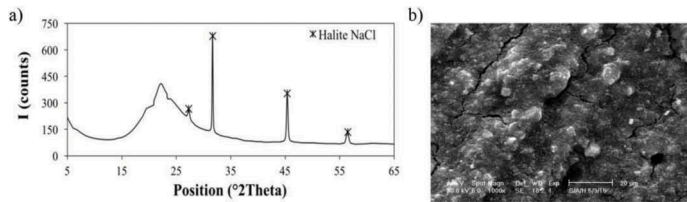


Figure 3. XRD chart (a) and SEM image of the nanosilica xerogel (b).

components are identifiable in the SEM image proposed in Figure 3b where the darker phase corresponds to the silica gel and the lighter one to the Halite crystals.

### 2.3 Grouted material

The specimens have been manufactured by pluviating the dry material in a mold and subsequently, aiming to guarantee treatment homogeneity and maximum saturation, the grout has been injected under a very low hydraulic gradient from the bottom to the top of the samples.

Aiming to study the evolution of the gelling process and fix the curing time of the specimens for the further mechanical tests, laboratory vane tests have been performed on samples after leaving them to cure for different periods. Several specimens have then been prepared with an initial void ratio of 0.8 and grouted with mix of different concentrations of silica obtained by adjusting the proportions between the components (see Table 2 where  $w_s$  represents the concentration in weight of silica over the total amount of grout).

The vane tests (ASTM 4648 2000) have been performed for each grout composition after different curing periods (from 3 hours to 28 days) ensuring the verticality of the vane during driving and rotation by means of a purposely conceived rail guide system (Figure 4a). The results of the experimental campaign shown in Figure 4b reveals a fast increase of the resistance approaching an almost stable condition after 28 days. The resistance strictly depends on the amount of injected silica with final values of shear strength equal to 240kPa, 530kPa and 680 kPa respectively for mixtures concentrations of 1.25%, 2.5% and 3.75% versus 30kPa recorded for the untreated material. In agreement with the results reported in Persoff *et al.* (1999), almost the 80% of the resistance is gained after about 5 days. Therefore, this curing time has been selected as standard for the mechanical tests hereinafter reported.

## 3 TRIAXIAL TESTS

### 3.1 Consolidated drained triaxial tests

The mechanical behavior of the treated and untreated sand has been initially studied by means of consolidated drained triaxial tests carried out at constant rate of deformation (5%/h) on cylindrical specimens (70x140mm) formed by compacting subsequent layers of 1 cm of thickness with a single blow of a 1kg weight falling from a height of 40cm. This procedure allowed to reach a void ratio ranging from 0.61 to 0.62 with a reasonable repeatability. In order to attain full saturation, carbon dioxide (more water soluble than air) was flushed before grouting from the bottom to the top of the specimens. Therefore, the samples were

Table 2. Composition of the grout mixes in the experiments of Figure 8.

ID	MasterRoc MP325 (%)	Water (%)	Accelerator (%)	$w_s$ (%)
1	25.00	58.30	16.70	3.75
2	16.70	66.60	16.70	2.51
3	8.30	75.00	16.70	1.25

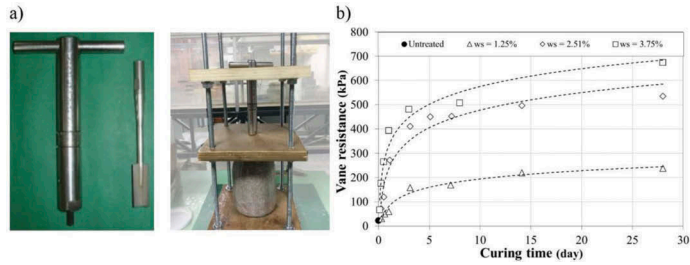


Figure 4. Laboratory vane test on the grouted samples: (a) equipment; (b) time increase of the vane shear resistance.

subjected to seepage with nanosilicate grout under low hydraulic gradient adopting different percentages among the compounds. After the prescribed curing time of 5 days the specimens were moved into a fully servo-controlled Bishop and Wesley triaxial apparatus where the back-pore water pressure was maintained to 600kPa during the tests to adsorb the remaining gas bubbles. Skempton B tests providing values higher than 0.98 proved that a sufficient degree of saturation was attained in all samples.

Figure 5a shows the results of three tests performed at 200kPa of effective confining pressure on natural sand and on specimens treated with different silica contents. It is worth noting that the treatment provides an increase of the peak shear strength with gains of 16% and 30% respect to the untreated material respectively for silica concentrations of 1.7% and 5.0%.

A more exhaustive assessment of the results shows a more brittle behavior of the treated material compared with the untreated one. All materials show the typical dilatant response with peak and softening. However, the grouted soil reveals larger dilation rates and this trend is increasing with the amount of injected silica. In the meantime, the post-peak softening becomes more evident for the treated soil, where is accompanied by a sudden stop of the volumetric deformation. These effects are clearly connected to the mechanisms of deformation acting into the material (see Figure 5c). In fact, despite the natural sand tends to deform in a more homogeneous way showing the typical barrel shape, the treated material reveals a tendency to localize deformations into shear bands that becomes more evident for higher silica content.

Finally, Figure 5b shows that the previous effects become more marked with time, suggesting that the improvement provided by the technique is likely larger than the one observed after 5 days.

### 3.2 Cyclic undrained triaxial tests

In order to prove the effectiveness of nanosilica grouting in reducing the liquefaction tendency of sand, a series of undrained triaxial cyclic tests were performed at constant strain ratio for different values of the cyclic stress ratio (CSR defined in Equation 1) at the confining pressure of 100kPa. The specimens were prepared at two different initial relative densities of 27% and 60% respectively by means of dry pluviation or dry tamping and when it was required treated with a grout containing the 5.0% in weight of silica nanoparticles. The response of the specimens was evaluated in terms of excess pore pressure ratio ( $r_u$  in Equation 2) and computing the number of cycles that triggers liquefaction ( $n_{liq}$ ). This state was defined as the condition where  $r_u=0.9$ .

$$CSR = \frac{q}{2\sigma'_{v0}} \quad (1)$$

$$r_u = \frac{\Delta u}{\sigma'_{v0}} \quad (2)$$

Where  $q$ =deviatoric stress;  $\Delta u$ =excess pore pressure;  $\sigma'_{v0}$ =initial effective vertical stress.

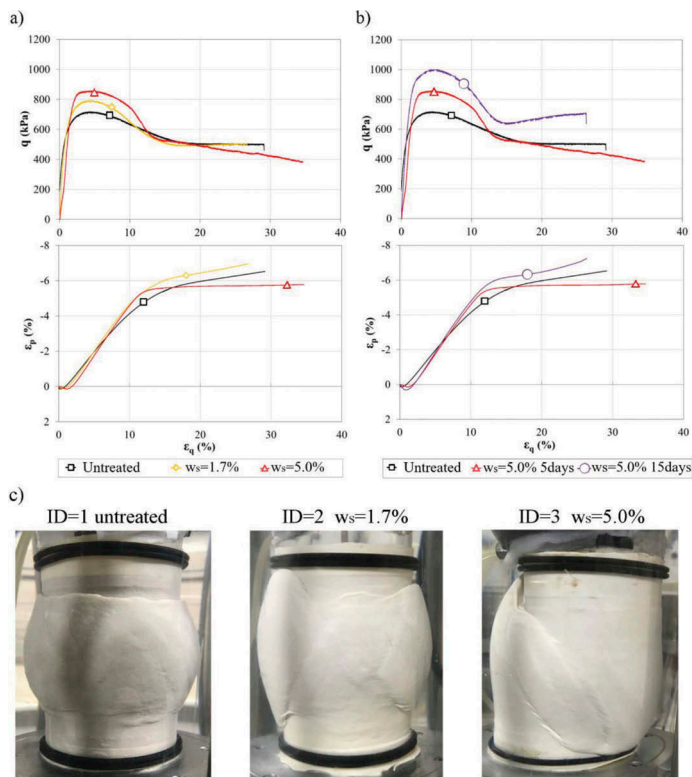


Figure 5. Monotonic triaxial tests on natural and grouted samples carried out with 200 kPa effective confining stress: (a) tests on the various materials after 5 days curing; (b) tests on sand grouted with 5% concentration of solid nanosilicate at different curing time; (c) pictures of the samples represented in Figure 5a at the end of the tests.

Figure 6 shows an example of results for untreated (6.a) and treated (6.b) specimens prepared at the same initial relative density of 60% and tested with a cyclic stress ratio of 0.5. In both tests the pore pressure increases gradually inducing a consequent reduction of the mean effective stress.

A more detailed analysis of the curves in the stress invariants plane reveals that the untreated specimen shows a continuous tendency to contract while the grouted specimen initially exhibits a tendency to dilate, and thus develop negative pore pressures, and subsequently starts to accumulate extrapressure in the further cycles with a much slower rate than the natural sand. The liquefaction condition is achieved after 15 cycles for the natural sand and after 58 cycles for the treated sand.

The outcomes of the whole experimental campaign are shown in Figure 7 for the dense (Figure 7a) and loose specimens (Figure 7b) plotting the number of cycles triggering liquefaction as a function of the applied cyclic stress ratio. The results clearly show a largely higher resistance to liquefaction of the grouted soil with respect to the natural sand. The results occur for both dense and loose specimens, since the number of cycles triggering liquefaction increases generally from three to four times between untreated and treated material.

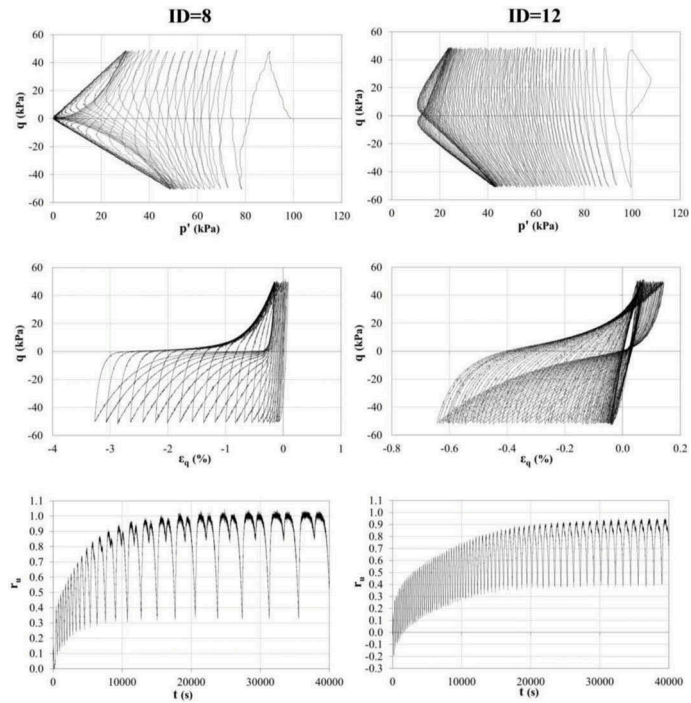


Figure 6. Liquefaction tests on natural (a) and treated ( $w_s=5\%$ ) sand (b) performed at 100 kPa initial effective confining stress ( $CSR=0.25$ ,  $e_0=0.62$ ).

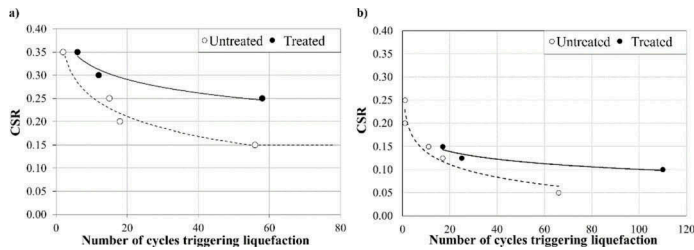


Figure 7. Cyclic undrained resistance on natural and grouted ( $w_s=5\%$ ) sand carried out with 100 kPa initial effective confining stress on relatively dense (a) and loose specimens (b).

#### 4 CONCLUSIONS AND FUTURE DEVELOPMENTS

The study herein described aims to investigate the effectiveness of low pressure injection of nanosilica to reduce the liquefaction susceptibility of sand. Thanks to its low viscosity, the nanosilica suspension could be easily injected into the soil by assigning low hydraulic gradient. After mixing with the activator, the gellification proceeds at a rate dictated by the relative composition of nanosilicate and activator ending with the formation of a compact gel that coats the soil grains and clogs the interparticle pores.

The initial study on the gelling process has demonstrated the flexibility of the technique by showing that the speed of the reaction may be tuned by controlling the amount of activator from a few minutes to several hours.



The vane tests carried out on specimens treated with grout prepared at various silica contents and cured with different periods have shown that the strength of the material increases with time and with the amount of injected silica.

The drained triaxial tests revealed an increase of peak strength and a more dilative and brittle response of the grouted sand with respect to the original material, being these effects more marked at higher silica contents.

Lastly, the undrained cyclic triaxial tests have confirmed that the presence of nanosilica reduces the tendency of the sand to accumulate pore pressure and therefore the treatment of soils ends in an increase of the liquefaction resistance.

## ACKNOWLEDGEMENTS

The authors wish to acknowledge the contribution by the EU funded project LIQUEFACT “Assessment and mitigation of liquefaction potential across Europe: a holistic approach to protect structures/infrastructures for improved resilience to earthquake-induced liquefaction disasters”, project ID 700748 funded under the H2020-DRS-2015.

## REFERENCES

- D’Appolonia, E., 1954. Symposium on dynamic testing of soils. ASTM International.
- Gallagher, P. M. and Mitchell, J. K. 2002. Influence of colloidal silica grout on liquefaction potential and cyclic undrained behavior of loose sand. *Soil Dynamics and Earthquake Engineering*, 22(9), pp. 1017-1026.
- Kirsch K. and Kirsch F., *Ground Improvement by Deep Vibratory Methods*, Second Edition, CRC press, 234 pp.
- Liao, H. J., Huang, C. C. and Chao, B. S. 2003. Liquefaction resistance of a colloid silica grouted sand. In: *Grouting and ground treatment*, pp. 1305-1313.
- Lyman, A. K. B. 1941. Compaction of cohesionless foundation soils by explosives. *Proceedings of the American Society of Civil Engineers*, 67(5), pp. 769-780.
- Mayne, P. W., Jones Jr, J. S. and Dumas, J. C. 1984. Ground response to dynamic compaction. *ASCE Journal of Geotechnical Engineering*, 110(6), pp. 757-774.
- Moridis, G. J. 1996. A field test of a waste containment technology using a new generation of injectable barrier liquids. *Spectrum* 96, pp. 18-23.
- Nguyen, T.V., Rayamajhi, D., Boulanger, R.W., Ashford, S.A., Lu, J., Elgamal, A., and Shao, L. 2012. Effects of DSM grids on shear stress distribution in liquefiable soil. *GeoCongress 2012, State of the Art and Practice in Geotechnical Engineering*, ASCE GSP 255, Oakland, CA, PP. 1948-1957.
- Persoff, P., Apps, J. A. and Moridis, G. J. 1999. Effect of dilution and contaminants on strength and hydraulic conductivity of sand grouted with colloidal silica gel. *ASCE Journal of Geotechnical and Geoenvironmental Engineering*, 125(6), pp.461-469.
- Salvatore, E., Modoni, G., Andò, E., Albano, M., Viggiani, C. 2017. Determination of the critical state of granular materials with triaxial tests. *Soils and Foundations*, 57(5), pp. 733-744.
- Seed, H. B. 1967. Analysis of soil liquefaction: Niigata earthquake. *Journal of the Soil Mechanics and Foundations Division*, 93(3), pp. 83-108.
- Traldi, D. and Levanto, P., 2016. *Metodi innovativi per il consolidamento e l'impermeabilizzazione in sotterraneo*. Ingegno, Volume 47.
- Yamauchi, T., Tezuka, H., and Tsukamoto, Y. 2017. Development of Rational Soil Liquefaction Countermeasure Consisting of Lattice-Shaped Soil Improvement by Jet Grouting for Existing Housing Estates. In *Geotechnical Hazards from Large Earthquakes and Heavy Rainfalls* (pp. 49-59). Springer, Tokyo.
- Yonekura, R. 1996. The developing process and the new concepts of chemical grout in Japan. Tokyo, pp. 889-901.